Desalination and Water Treatment
www.deswater.com

doi: 10.5004/dwt.2017.11465

64 (2017) 279–286
February

Investigations of a membrane distillation pilot plant with a capillary module

Marek Gryta

West Pomeranian University of Technology, Szczecin, Faculty of Chemical Technology and Engineering, Pułaskiego 10, 70-322 Szczecin, Poland, email: marek.gryta@zut.edu.pl

Received 10 May 2016; Accepted 6 August 2016

ABSTRACT

The effectiveness of work of a 2-inch capillary module, with membrane area equal to 0.71 m^2, in a pilot plant for direct contact membrane distillation was investigated. The module was designed with application of polypropylene membranes Accurel PP S6/2 with diameter of 1.8/2.6 mm and effective length of 1.05 m. Membranes placed inside the tubular shell were assembled in a form of braids, using three capillaries in each braid, obtaining the packing density coefficient of 31%. This configuration ensured good conditions of stream mixing on the shell side, and as a result, the effectiveness of module operation was close to results obtained for smaller capillary modules in the laboratory tests. The permeate flux at the used parameters of membrane distillation (T_F = 355 K) was above 25 L m^{-2} h^{-1}, and the energy consumption was at a level of 23.4 kW m^{-2} of membranes (936 kWh m^{-3} of distillate), while the thermal efficiency of process amounted to 70%–80%.

Keywords: Membrane distillation; Module design; Thermal efficiency; Desalination

1. Introduction

In membrane distillation (MD) process, volatile species in the hot feed vaporize at a hydrophobic membrane surface and form vapour permeates, which pass through the pores filled only by gas phase [1–3]. The vapour condensation takes place either inside or outside the membrane module, depending on the MD variant [4]. In the case of direct contact MD (DCMD), the vapour is condensed at the membrane/cold liquid (cooled distillate) interface inside the MD module [1–4]. The vapour can be also condensed on a cooled plate, which is separated from membrane by air gap (air gap MD – AGMD) [4–7].

The separation mechanism, occurring in the MD process, makes the non-volatile components, such as salts, retained nearly in 100%; thus, the MD can be used for production of fresh water, even from brines [7–10]. Moreover, the MD process was successfully applied for water and wastewater treatment, for food processing and water recovery from different industrial effluents [4,5,11].

The driving force for the mass transfer in MD process is the vapour pressure difference across the membrane, which depends on the temperature and feed composition at the membrane walls [6,7,12]. The occurrence of simultaneous heat and mass transfer generates the polarization effects in boundary layers. The increase of flow velocity reduces the thickness of boundary layers formed in the membrane module channels, and hence decreases the polarization phenomenon [13–15]. For this reason, the permeate flux depends, to a high extent, on a feed temperature and the streams flow rates in the MD module [4,12–18].

The creation of appropriate hydrodynamic conditions inside the MD module is significantly affected by the module design and the MD configuration [4,12,16,17]. There are three major MD module configurations, including plate-and-frame module, spiral wound membrane module and tubular or shell-and-tube module. The last type of configuration is assembled using the capillary membranes; thus, this design is also named the capillary module. In these modules, a bundle of porous capillaries is arranged into a tubular shell, like in a tube-and-shell heat exchanger configuration [16–18]. The capillary modules are more beneficial than plate-and-frame modules, fabricated with flat sheet membranes, because they

Presented at the conference on Membranes and Membrane Processes in Environmental Protection (MEMPEP 2016), Zakopane, Poland, 15–19 June 2016.

can be packed at much higher membrane area to a module volume ratio.

The availability of commercial MD modules is one of the limitations of industrial implementation of the MD process. In the recent years, several kinds of MD modules have been developed and applied in pilot plants construction [4–7,12,16]. The majority of these modules are based on the AGMD design, which have the additional channel for cooling water enabling the recovery of latent heat. This allows to enhance the effectiveness of energy consumed in MD process several times [4,12]. The energy transferred from the feed to distillate can be additionally recovered in an external heat exchanger, as in the case of plate-and-frame AGMD modules design, manufactured by Scarab Development AB and XZero AB (Sweden) [16,19]. This solution consists of an AGMD module. In this design, the cold saline water flows through a condenser with non-permeable walls, what increases its temperature, due to the vapour condensation. Subsequently, the saline water (feed) passes through an external heat exchanger, where an additional heat is added before the feed is returned into the module. A similar conception using Memstill technology (capillary membranes) was designed by TNO (The Netherlands Organisation for Applied Scientific Research), Keppel Seghers (Belgium), and Aquastill (The Netherlands) [4,20,21].

Spiral-wound AGMD modules with an integrated heat recovery for different solar-powered desalination systems have been developed since 2003 by Fraunhofer Institute for Solar Energy System (ISE) and Solar Spring GmbH (Germany). The pilot installations were localized in the Island of Gran Canaria in Spain; Jordan, Egypt, Mexico, and Pantelleria in Italy; Aqaba in Jordan; and Amarika in Namibia [12,22,23]. The internal heat recovery was also introduced by Memsys (Germany and Singapore) and Aquaver (The Netherlands): The Memsys system is based on vacuum enhanced multieffect AGMD variant, incorporating heat recovery and recycling in a plate-and-frame membrane module [4,24].

In the pilot plants with the above-mentioned modules, the yield of MD at a level of 2–7 L m^{-2} h^{-1} was obtained [5,12,22,23]. A larger yield (over 20 L m^{-2} h^{-1}) can be achieved using the capillary modules in DCMD configuration [17,18]. However, a significant fraction of energy is lost in this case, due to the heat conduction through the membranes [13,15]. An enhancement of the effectiveness of energy utilization (up to 70%–80%) was obtained at the feed temperature above 353 K [25], which also enabled the application of the external system for heat recovery [18,26,27].

A vapour transport resistance is inversely proportional to the membrane thickness; thus, the thin membranes (50–80 μm), supported by polymeric nets, are used in presented industrial MD modules [12,16,28]. During the studies of water desalination in pilot plants, the intensive scaling of the membranes was found [21,23]. As a result, a fraction of membrane pores became wetted, what resulted in a leakage of the feed into distillate and in deterioration of fresh water produced [5,15,23]. Moreover, the removal of deposits, for example, by module rinsing with acid solutions, was required [23] what even increased the rate of membrane wetting [29]. In such cases, the intensity of membrane wetting can be limited by application of the capillary membranes with thicker walls [9].

In capillary DCMD modules, it is necessary to ensure good flow conditions also on the shell side. In order to increase the flow turbulence between capillaries, mixing elements are assembled, or membranes are arranged in a proper shape (e.g., twisted, braided and wave) causing considerable turbulence of liquid flow [16–18,24,30]. These solutions may reduce the temperature polarization effect and enhance permeate fluxes in MD modules.

Due to the evaporation, the feed temperature rapidly decreases along with the MD module length, what reduces the yield of industrial (long) modules. For this reason, the dimension of channels between membranes should have the hydraulic diameter of at least 2–3 mm (higher heat capacity of stream) [17,24,30]. With regard to this, a value of capillary packing density in MD modules should amount to 0.3–0.6 [17,18,31]. However, the presence a free volume between capillaries causes their random arrangement in the shell. This leads to a range of duct sizes and shapes in the shell, or the module shows a certain extent variation of the local packing fraction [17,31,32]. In order to limit the capillaries arrangement changes inside the shell, such a configuration of capillaries should be applied, which prevents their free displacements. Good results were obtained by assembling capillaries inside sieve baffles or by a tight packing of membranes in a form of braided capillaries [17,18]. The most advantageous operating conditions of MD module were obtained with membranes arranged in a form of braided capillaries, because the shape of braided membranes acted as a static mixer around the fibres, and as a consequence, the module yield was over doubly enhanced [16–18,30].

In the presented work, the effectiveness of exploitation of 2-inch capillary module, inside of which the membranes arranged in the form of braided capillaries were assembled, was studied.

2. Experimental setup

2.1. DCMD module design

The capillary modules made of Accurel PP S6/2 (Membrana GmbH, Germany) polypropylene membranes were used in the studies. The capillary diameters were 1.8/2.6 mm; nominal and maximum diameters of pores were 0.2 and 0.6 μm, respectively; and the open porosity was 73% (manufacturer's data). Membranes were assembled in modules arranged in the form of braided capillaries, three capillaries in each braid. Parameters of particular modules are presented in Table 1, and their construction is schematically shown in Fig. 1. The membrane area was calculated based on the inner diameter of used membranes. The MK1 module was made from PVC tube with the internal diameter of 2 inches. Diameters of side connectors (4) amounted to ¾ inch, whereas diameters of connectors fixed to the module head (5) were equal to 1 inch. Membranes were attached from both sides in 6 cm thicker resin pots (2). An effective membrane length in the MK1 module was equal to 1.05 m.

Yields of MD process obtained for small laboratory modules are usually significantly higher than those obtained for larger units in the pilot plant studies [12,15]. In order to demonstrate the reason of this decrease in the yield, additional studies were carried out with modules having smaller diameters (MK2–MK4).

By increasing the shell diameter, an increase of non-uniform distribution of the flow rates of liquid between the capillary membranes should be expected, what can result

Table 1
Capillary module parameters

Module	Diameter (m)	Length (m)	Area (m^2)	Capillaries (no.)	Packing density (%)	Shell
MK1	0.051	1.05	0.710	120	31	PVC
MK2	0.007	1.0	0.017	3	41	PVC
MK3	0.018	0.58	0.059	18	38	PVC
MK4	0.021	0.95	0.113	21	32	Glass

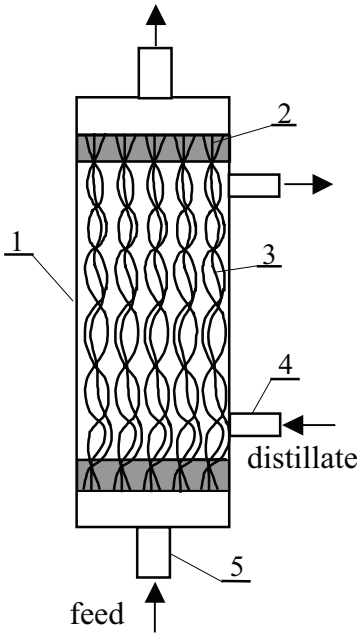

Fig. 1. DCMD capillary module.
Note: 1 – shell, 2 – resin pots, 3 – braided capillary membranes, and 4 and 5 – connectors.

in the module efficiency reduction. In order to investigate a significance of this phenomenon for the MK1 module, additional studies were carried out with a module having a small diameter (MK2), in which only one braid was assembled. The studies of hydrodynamic conditions on the shell side were also performed using a coloured impulse method (module MK4).

A variation of a stream temperature along a module decreases the driving force; thus, larger permeate fluxes are achieved for shorter modules in the MD process. For this reason, the results obtained for the MK1 module were compared with those obtained for two times shorter module (MK3).

2.2. DCMD pilot plant

The design of MD pilot plant is schematically presented in Fig. 2.

Principal elements of the pilot plant were: feed tank (12 m^3), distillate tank (2 m^3), impeller pumps with elevation head of 35 m H_2O, stainless steel heat exchangers, 100 μm screen filters, and orifice for the measurement of liquid flow rates. Tanks, valves and a part of pipes were made of steel coated with a layer of rubber. The majority of pipelines were made of polyethylene. The pilot installation was constructed based on the existing factory's infrastructure; thus, its capacity was overestimated in

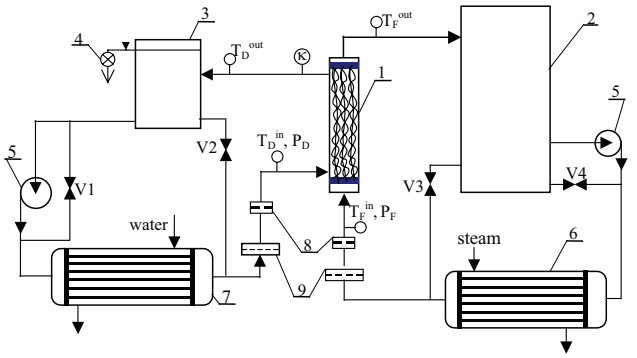

Fig. 2. DCMD pilot plant.
Note: 1 – MD module, 2 – feed tank, 3 – distillate tank, 4 – distillate flow meter, 5 – pump, 6 and 7 – heat exchanger, 8 – orifice, 9 – filter, T – temperature, P – pressure, and k – conductivity.

comparison with one MK1 module; therefore, bypasses were used (valves V1–V4). On the other hand, the possibility of connection of several additional MD modules was created.

The MK1 module was assembled in a vertical position. The feed and distillate streams flowed concurrently from the bottom to the upper part of the module. The feed circulated inside the capillary membranes. The distillate temperature at the entrance of the module was kept at a constant level of 293 ± 5 K, whereas the feed temperature was in the range of 333–363 K. Flow rates within the range 0.2–1.4 m s^{-1} were used during measurements. The tap water with HCl addition (pH = 4.5) was used as a feed.

2.3. MD laboratory studies

MD studies in the laboratory scale were performed using the experimental setup shown in Fig. 3. The installation consisted of two thermostatic cycles (feed and distillate). The inlet temperature of distillate (293 K) was constant during all experiments, while feed temperatures were varied in the range of 333–358 K. Stream temperatures were measured using thermometers with 0.2 K accuracy. During experiments, the feed was supplied into capillaries (0.0075–0.014 L s^{-1}), whereas the distillate flowed on the shell side of the MD module (0.008–0.014 L s^{-1}). Similarly as in the pilot plant, the tap water was used as a feed.

During MD experiments, the excess volume of distillate was continuously measured. The obtained permeate flux was calculated on the basis of the distillate volume changes over studied period of time (Eq. (1)):

$$J = \Delta V/A\,\Delta t \quad (1)$$

where ΔV is an excess of distillate volume during the Δt period, and A is module area.

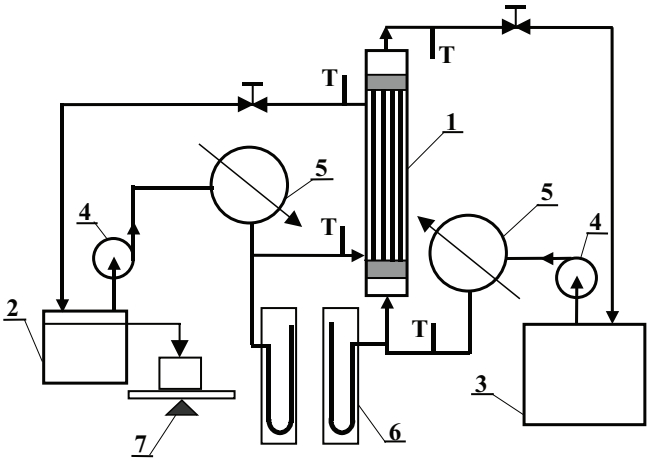

Fig. 3. DCMD experimental setup.
Note: 1 – MD module, 2 – distillate tank, 3 – feed tank, 4 – pump, 5 – heat exchanger, 6 – manometer, 7 – balance, and T – thermometer.

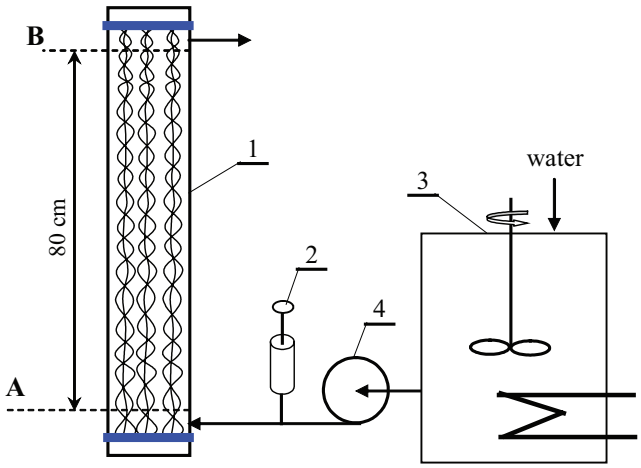

Fig. 4. Experimental setup used for hydrodynamic studies.
Note: 1 – MD module, 2 – dye dosing, 3 – thermostat, and 4 – peristaltic pumps.

The heat used effectively in DCMD is the energy consumed as the latent heat (Q_V) for water vapour production, whilst the heat transferred by conduction across the membrane is considered as a heat loss. The heat efficiency (η_T) was calculated using Eq. (2):

$$\eta_T = \frac{Q_V}{Q_T} = \frac{J_V H_V A}{(T_F^{in} - T_F^{out}) m_F c_P} \quad (2)$$

where Q_V is the latent heat; Q_T is the total heat consumed in MD process, T_F^{in} and T_F^{out} are feed temperatures at MD module inlet and outlet; H_V is latent heat of evaporation; c_P is the specific heat; and m_F is the feed mass flow.

2.4. Hydrodynamic studies

The installation used for studies of residence time distribution (RTD) inside the shell side of capillary module is presented in Fig. 4. Thermostatic tap water (298 K) was supplied to a vertically arranged module MK4 by peristaltic pump. For a given flow rate, the water flow through a module lasted at least 5 min; subsequently, a dye was introduced into a water stream by a syringe, obtaining a coloured impulse. Measurement lines A (initial) and B (final) were located 5 cm from shell inlets, and a distance between the A and B lines amounted to 80 cm. A time of coloured water flow from A to B line ($t_{INITIAL}$) and the time of coloured water outflow from B line (t_{FINISH}) were measured. The measurement time was started when the A line was crossed by the coloured water. The maximal length to which the water layer was coloured during the flow through the module (coloured axial length) was also measured.

3. Results

3.1. Flow conditions on the shell side

The analysis of RTD is a good indicator of the hydrodynamic conditions in a module. In an ideal hollow fibre module (plug flow), the value of liquid flowing time through the module should be close to the calculated RTD value [33]. The results of studies (two series) of RTD for a coloured impulse in the MK4 module are shown in Fig. 5. The RTD value was

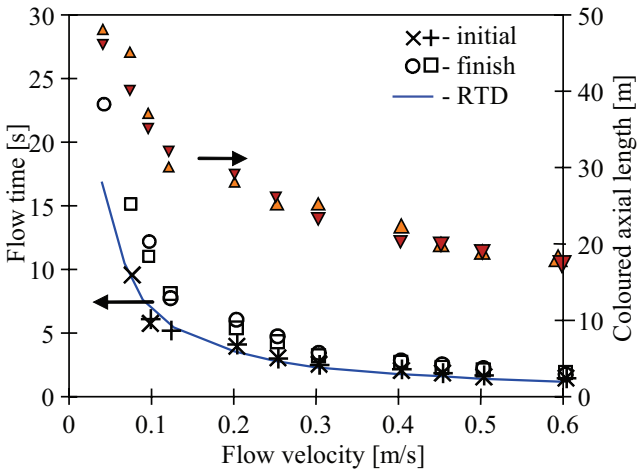

Fig. 5. The influence of flow rate on the residence time distribution of dye inside the MK4 module and length of coloured water. RTD – values calculated for plug flow.

calculated for assumed plug flow, taking into account a value of membrane packing density equal to 32% (MK4).

The obtained results confirmed that in an actual shell-side flow the distribution of fluid across the capillary bundle tended to broaden the measured RTD. For all studied flow rates, the residence time of dye in the module was longer than the calculated values of RDT. Particularly, large difference occurred for flow rates smaller than 0.2 m s^{-}. In this case, it was also observed that a part of coloured water was outflowing from the module significantly faster than the calculated RTD value. Such results may indicate the possibility of non-uniform distribution of capillaries inside the shell, which caused the formation of channels with different dimensions [17,31,32]. The water flows faster in wider channels (between capillaries) than it is indicated by the calculated average velocity. During the coloured water flow along the module, due to a radial dispersion and diffusion, a dye flowing along the wall of capillaries also penetrated faster flowing streams (channels between the capillaries), and as a result, the water

was uniformly coloured throughout the entire cross section of the module, after it flowed the axial distance of 15–20 cm.

Visual observations of coloured streams performed for a very low flow velocity (0.1–0.2 m s^{-1}) revealed reasons of flow rates distribution. The results of these observations are schematically presented in Fig. 6. In a laminar flow, the coloured water stream was flowing into the module and flowed around the membranes in a swirling motion, what additionally decreased the axial velocity in this zone. Flow resistances in void spaces among capillaries were smaller, what enabled to achieve larger flow rates in comparison with the average value. Similar results were obtained during studies of flow and axial dispersion in a sinusoidal-walled tube [34], the shape of which resembled in a certain extent the channel created by braided capillaries.

The occurrence of different values of flow velocity in the module cross-section caused that an axial thickness of layer of coloured water increased to almost 50 cm for the smallest calculated average flow velocity. The thickness of this layer was reduced to 17 cm, while the flow velocity was increased to 0.6 m s^{-1} (Fig. 5). At flow rates higher than 0.3 m s^{-1}, the stream coloured by dye, after flowing into the module, coloured uniformly the water through the entire cross-section of the module, after flowing an axial distance equal to 4–6 cm. This result confirmed a good action of braided capillaries as the static mixer [16,17,30]. Due to an increase in the flow rate, the increase in the turbulence of water flow in the module caused the faster dye washing out also from narrow channels. Therefore, the residence time of liquid in the module for larger velocities (v > 0.4 m s^{-1}) was closer to the average value (RDT) – Fig. 5.

Moreover, an elongation of the residence time of the dye in the module was observed at flow rates higher than 0.5 m s^{-1}. This was associated with growing intensity of liquid mixing in their interior. It was observed that the flow turbulence increased along with the increase of flow rates. As a result, a part of coloured water was transferred backwards, what caused the colouration of new portion of water, for example, for v_F = 0.6 m s^{-1} the axial length of coloured water was equal to 17 cm (Fig. 5). Due to growing volume of coloured water, an apparent longer residence time in the module was noticed.

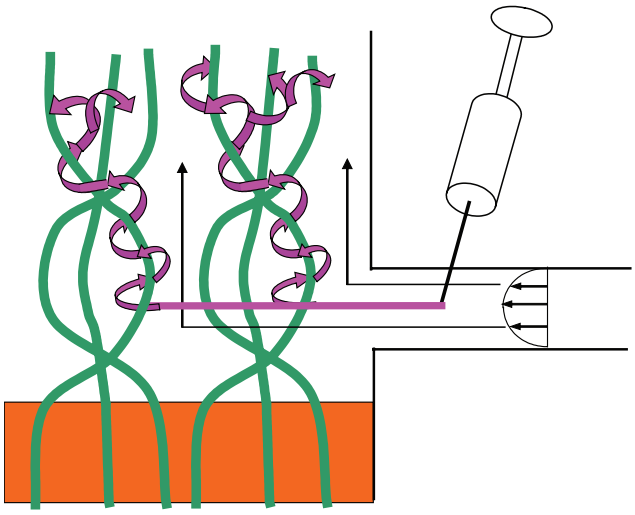

Fig. 6. Streams distribution inside the module with braded capillaries.

3.2. The influence of flow velocity on the module yield

The module efficiency mainly depends on the flow conditions of feed and distillate for applied temperatures of streams [35,36]. Energy necessary for the evaporation is collected from the feed stream; thus, flow rates of the feed have a larger influence on the magnitude of the permeate flux as it was confirmed by the results presented in Fig. 7. As a consequence of heat and mass transfer in the MD process, solutions temperatures vary alongside the module, what results in a decline of the module efficiency [12–14,26,28]. For tested MK2 module, the temperature of the feed after flowing a distance of 1.0 m was decreased by 10–20 K. A temperature at the module outlet became closer to the inlet temperature along with the increase of the flow rate, what limited a decline of the driving force along the module length [15,28].

In the studied case (MK2), an enhancement of the distillate flow rates from 0.25 to 0.75 m s^{-} caused that the permeate flux was increased only by 5%–10%. With regard to an exponential character of vapour pressure dependence on the permeate flux, the temperature changes on the distillate side have a smaller influence on the value of the permeate flux [5,14]. However, in the case of non-uniform radial disturbance of the flow rate, the distillate temperature may be locally high, for example, 333 K, what causes even twofold to threefold decrease of the module yield [16,17].

Moreover, the membrane surface temperature declines significantly on the feed side, due to the water vaporization, and increases on the distillate side, due to the vapour condensation during the MD process [15,23,36]. This phenomenon is known as a temperature polarization and may be reduced by increasing the convective heat transfer coefficients, which are strongly affected by a flow turbulence, characterized by Reynolds number (*Re*). The value close to *Re* = 3,000 (v_F = 0.6 m s^{-1}) allowed to eliminate significantly the effect of polarization and the permeate flux was stabilized (Fig. 7). For this reason, a further increase of the flow rate is not advisable (for used Accurel PP S6/2 membranes). Moreover, in the

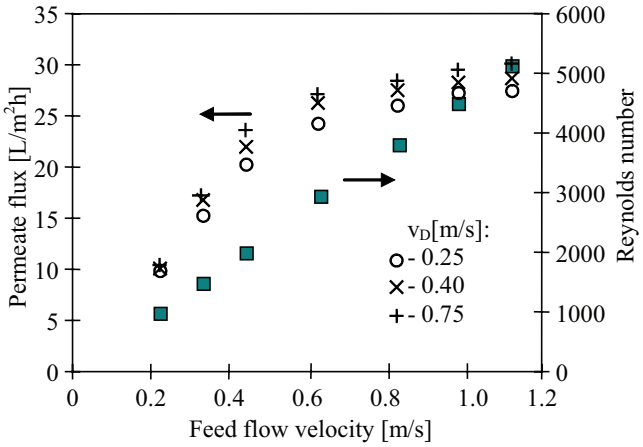

Fig. 7. The influence of feed flow velocity on the permeate flux and Reynolds number (on the feed side). MK2 module. Inlet feed and distillate temperature 353 and 293 K, respectively.

case the lower feed temperatures (below 333 K), an excessive increase of the flow rate mainly improves the conditions of heat transfer through the membrane, thereby increasing the energy losses in the MD process [15].

Along with the increase of the flow rate, the hydraulic pressure also increases and may accelerate the membrane wetting. Due to a risk of membrane wettability, the pressure difference on both sides of the used Accurel PP S6/2 membranes should not exceed 2×10^5 N m^{-2} [18,37]. The value of pressure amounted to 1.8×10^5 N m^{-2} in the pilot MD installation was obtained for the feed flow rate inside the module MK1 equal to 1.4 m s^{-1}. The hydraulic pressure on the feed side and the distillate side was adjusted in such a way, so it would have a similar value during the operation of the MD installation. However, risk of membrane wettability appears, when the flow in one of the cycles will be stopped due to various reasons.

The results obtained for the MK1 module in the pilot plant and for smaller modules tested under the laboratory conditions are presented in Fig. 8. In each case, the largest changes in the yield occurred for the flow rate below 1 m s^{-1}. The highest values of the permeate flux were achieved for the shortest module MK3 (L = 0.53 m), what confirmed that module length shortening allowed to obtain a larger permeate flux [34]. However, the temperature difference between the inlet and the outlet of the module decreased along with the increase of the flow rate. Therefore, for higher flow velocity (v_F > 1.2 m s^{-1}), the permeate flux obtained for the twofold longer MK2 module was close to that obtained for MK3 module.

The permeate flux obtained for MK1 module, tested in the pilot plant installation, was smaller than the one obtained for MK2 and MK3 modules (Fig. 8). For the flow rate of 1.2 m s^{-1}, and inlet temperature of the feed equal to 353 K, the yield of the MK1 module amounted to 24.6 L m^{-2} h^{-1}; thus, it was 13% lower in comparison with one obtained for modules tested in laboratory conditions. Moreover, a relative stabilization of yield growth (similarly as for the MK2 and MK3 modules) was obtained for flow rates larger than 1 m s^{-}, but only for a lower feed temperature (Fig. 8 – 338 K). Flow turbulence on the feed side in each module was similar; thus, the obtained results indicated a slight unevenness of the flow on the distillate side [24]. This problem grows together with the increase of diameter of capillary module. For this reason, the axially assembled perforated tube was used for liquid distribution in the capillary MD modules with larger diameters [18].

3.3. The influence of the feed temperature on the permeate flux

Variations of the efficiency of MD modules as a function of feed temperature presented in Fig. 9 indicate that the curve N=f(T) exhibits an exponential character, which results of the dependence of water vapour partial pressure on the temperature [12,14,36]. In some cases (in modules with poor mixing), a linear dependence of yield on the temperature is observed, due to a negative interaction of the temperature polarization. The MK1 module, similarly as the MK2 module tested in laboratory conditions, demonstrated an exponential growth of yield, particularly for the feed temperature above 348 K. The obtained results confirmed that a tested design with braided capillaries ensured good hydrodynamic conditions in 2-inch module, which was also demonstrated in other works concerning the module with smaller dimensions [4,17,18].

3.4. Studies of the thermal efficiency

In classical heat exchangers, a counter-current flow allows to exchange a larger amount of energy. However, in the case of MD module, the heat conducted by the membrane is considered as an energy loss. However, in several works, there have been demonstrated that such a direction of streams flows allows to enhance the MD module yield [13]. The results presented in Fig. 10 (MK4 module, L = 0.95 cm) indicated that in the case of longer MD module, the application of counter-current flow resulted in a small increase in the permeate flux, due to the significant changes of the bulk temperature. However, this allowed to enhance the thermal efficiency of module, which was increased from 75% to 80% for temperature of 363 K.

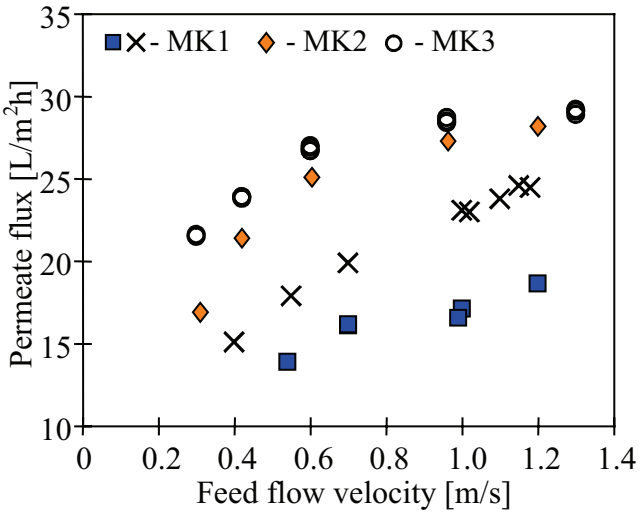

Fig. 8. The influence of feed flow velocity on the permeate flux. T_F = 353 K (x, ○, ♦) and 338 K (■), T_D = 293 K, and v_D = 0.38 m s^{-1}.

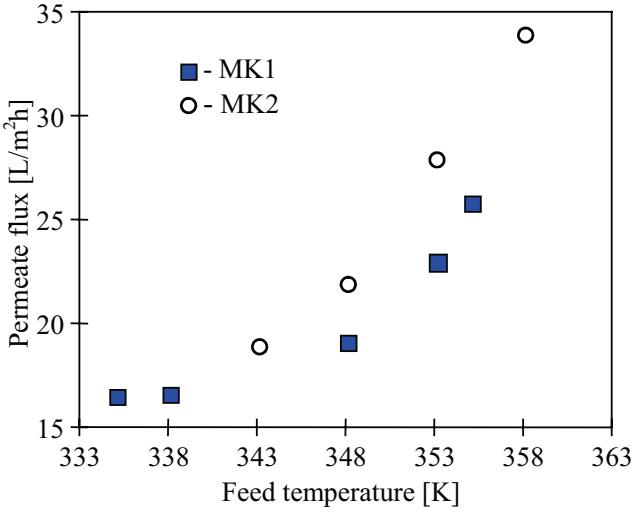

Fig. 9. Dependence of the permeate flux on inlet feed temperature for MK1 and MK2 modules. Flow velocity: v_F = 1 m s^{-1}, v_D = 0.4 m s^{-1}. T_{Din} = 293 K.

Moreover, the thermal efficiency significantly increased along with the feed temperature. This resulted of a fact that the permeate flux increased exponentially along with increase of temperature (Fig. 9) and due to an intensive mass transfer (evaporation), which also caused an increase of the temperature polarization [15,24]. The later phenomenon reduced a value of ΔT across the membrane [24], and as a result, the amount of conducted heat (heat losses) was reduced (Fig. 11). It is worthy to notice that a greater efficiency of MD was achieved, due to an exponential dependence of vapour pressure on temperature, for smaller temperature differences across the membrane, but for high temperatures of streams. For example, the higher permeate flux would be obtained for T_F = 353 K and T_D = 333 K (ΔT = 20 K) than in the case with larger temperature differences (e.g., T_F = 333 K, T_D = 293 K, thus ΔT = 40 K).

The studies performed in the pilot plant confirmed that advantageous hydrodynamic conditions, existing in the studied capillary modules, permitted to achieve both a higher efficiency of the MK1 module and a beneficial ratio of energy consumed for the mass transport in relation to the total energy consumed in the process. The determined thermal efficiency of MK1 module was in the range from 60% to 70% (Fig. 12).

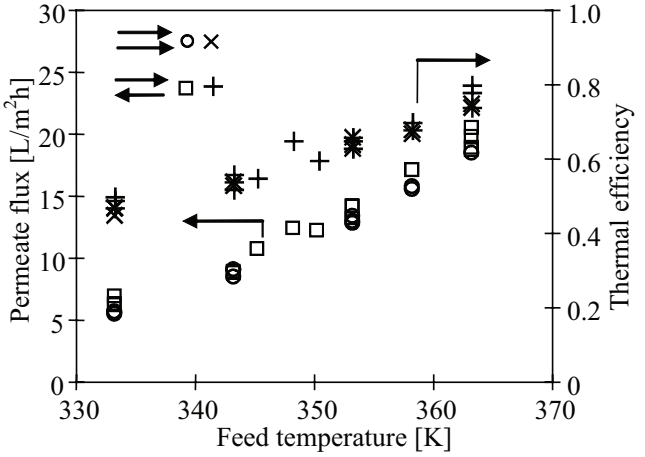

Fig. 10. The effect of concurrent and counter-current flow for different feed temperatures. MK4 module. Flow velocity v_F = 0.31 m s^{-1}, v_D = 0.25 m s^{-1}. T_{Din} = 293 K.

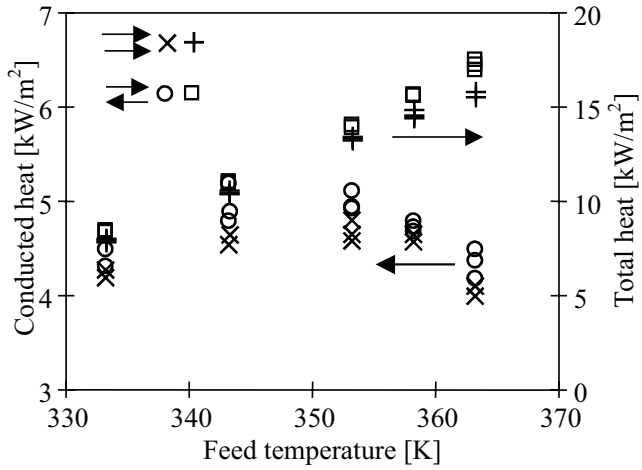

Fig. 11. The effect of concurrent and counter-current flow for different feed temperatures on total and conducted heat values. MK4 module. Flow velocity: v_F = 0.31 m s^{-1}, v_D = 0.25 m s^{-1}. T_{Din} = 293 K.

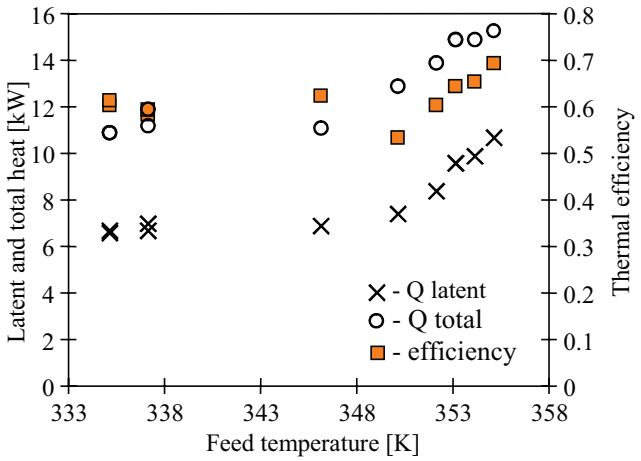

Fig. 12. The effect of feed temperature on heat consumption and thermal efficiency of MK1 module studied in the pilot plant.

In the MD process, significant amounts of energy with regard to water evaporation are consumed. In the studied case, the feeding of MK1 module required supply of almost 15.3 kW of energy that was about 23.4 kW m^{-2} of membranes (T_F = 355 K). The permeate flux amounted to about 25 L m^{-2} h^{-1}, under this conditions; thus, 936 kWh was consumed to produce 1 m^3 of distillate. This result indicated that a tested design of capillary module exhibited a high efficiency, because in other works, almost 1,300 kWh m^{-3} was consumed [4]. In the case of MK4 module, tested at laboratory conditions (Fig. 9), the electrical power requirement at a level of 835 kWh m^{-3} was obtained. A similar energy consumption (810 kWh m^{-3}) was reported using the AGMD module of Scarab Development AB (Sweden) [5]. However, even in the case of recovery of condensation heat, the energy consumption is still high (55–130 kWh m^{-3}) [11,12], what gives the cost above 5 $ m^{-3} of fresh water. This cost is significantly higher than that incurred during the water desalination by reverse osmosis (RO) [4,20]. Therefore, one should not expect that in the coming years, the MD process would replace RO. However, in some regions (arid zone), the application of RO is practically impossible (e.g., brine as a water source), and in such cases, the utilization of MD process can be taken into consideration [8–10].

4. Conclusions

The examined 2-inch capillary module demonstrated the usefulness for exploitation at the industrial conditions. The achieved efficiency of module studied in DCMD pilot plant installation was close to values obtained in laboratory modules.

The feed temperature has a significant influence on the MD process efficiency, and its value was improved by using a higher feed temperature. The permeate flux equal to 25 L h^{-1} recalculated to 1 m^2 of the membrane, and the thermal efficiency over 70% were achieved for the feed temperature equal to 355 K.

The MD process requires a supply of a large amount of energy, which causes high operational costs. For this reason, the use of MD process for water desalination can find the application in particular cases, such as fresh water production from brines.

Acknowledgement

The National Science Centre, Poland, is acknowledged for the support of this work (DEC-2014/15/B/ST8/00045).

References

[1] M.M.A. Shirazi, A. Kargari, M. Tabatabaei, Evaluation of commercial PTFE membranes in desalination by direct contact membrane distillation, Chem. Eng. Proc.: Process Intensification, 76 (2014) 16–25.
[2] M. Gryta, Wettability of polypropylene capillary membranes during the membrane distillation process, Chem. Pap., 66 (2012) 92–98.
[3] M. Bhadra, S. Roy, S. Mitra, Flux enhancement in direct contact membrane distillation by implementing carbon nanotube immobilized PTFE membrane, Sep. Purif. Technol., 161 (2016) 136–143.
[4] P. Wang, T.S. Chung, Recent advances in membrane distillation processes: membrane development, configuration design and application exploring, J. Membr. Sci., 474 (2015) 39–56.
[5] E. Guillén-Burrieza, J. Blanco, G. Zaragoza, D.-C. Alarcón, P. Palenzuela, M. Ibarra, W. Gernjak, Experimental analysis of an air gap membrane distillation solar desalination pilot system, J. Membr. Sci., 379 (2011) 386–396.
[6] Q. He, P. Li, H. Geng, Ch. Zhang, J. Wang, H. Chang, Modeling and optimization of air gap membrane distillation system for desalination, Desalination, 354 (2014) 68–75.
[7] A. Alkhudhiri, N. Darwish, N. Hilal, Membrane distillation: a comprehensive review, Desalination, 287 (2012) 2–18.
[8] F. Edwie, T.S. Chung, Development of simultaneous membrane distillation–crystallization (SMDC) technology for treatment of saturated brine, Chem. Eng. Sci., 98 (2013) 160–172.
[9] M. Gryta, M. Palczyński, Desalination of geothermal water by membrane distillation, Membr. Water Treat., 2 (2011) 147–158.
[10] J. Xiaosheng, E. Curcio, S. Al Obaidani, G. Di Profio, E. Fontananova, E. Drioli, Membrane distillation-crystallization of seawater reverse osmosis brines, Sep. Purif. Technol., 71 (2010) 76–82.
[11] X. Li, Y. Qin, R. Liu, Y. Zhang, K. Yao, Study on concentration of aqueous sulfuric acid solution by multiple-effect membrane distillation, Desalination, 307 (2012) 34–41.
[12] D. Winter, J. Koschikowski, M. Wieghaus, Desalination using membrane distillation: experimental studies on full scale spiral wound modules, J. Membr. Sci., 375 (2011) 104–112.
[13] Ch.-D. Ho, H. Chang, T.-J. Yang, K.-Y. Wu, L. Chen, Theoretical and experimental studies of laminar flow hollow fiber direct contact membrane distillation modules, Desalination, 378 (2016) 108–116.
[14] A.E. Khalifa, Water and air gap membrane distillation for water desalination – an experimental comparative study, Sep. Purif. Technol., 141 (2015) 276–284.
[15] L. Francis, N. Ghaffour, A.S. Alsaadi, S.P. Nunes, G.L. Amy, Performance evaluation of the DCMD desalination process under bench scale and large scale module operating conditions, J. Membr. Sci., 455 (2014) 103–112.
[16] E. Drioli, A. Ali, F. Macedonio, Membrane distillation: recent developments and perspectives, Desalination, 356 (2015) 56–84.
[17] M. Gryta, M. Tomaszewska, A.W. Morawski, A capillary module for membrane distillation process, Chem. Pap., 54 (2000) 370–374.
[18] K. Schneider, W. Hölz, R. Wollbeck, S. Ripperger, Membranes and modules for transmembrane distillation, J. Membr. Sci., 39 (1988) 25–42.
[19] A. Kullab, A. Martin, Membrane distillation and applications for water purification in thermal cogeneration plants, Sep. Purif. Technol., 76 (2011) 231–237.
[20] K. Tarnacki, M. Meneses, T. Melin, J. van Medevoort, A. Jansen, Environmental assessment of desalination processes: reverse osmosis and Memstill®, Desalination, 296 (2012) 69–80.
[21] J.H. Hanemaaijer, J. van Medevoort, A.E. Jansen, Ch. Dotremont, E. van Sonsbeek, T. Yuan, L. De Ryck, Memstill membrane distillation – a future desalination Technology, Desalination, 199 (2006) 175–176.
[22] R. Schwantes, A. Cipollina, F. Gross, J. Koschikowski, D. Pfeifle, M. Rolletschek, V. Subiela, Membrane distillation: solar and waste heat driven demonstration plants for desalination, Desalination, 323 (2013) 93–106.
[23] F. Banat, N. Jwaied, Autonomous membrane distillation pilot plant unit driven by solar energy: experiences and lessons learned, Int. J. Sustain. Water Environ. Syst., 1 (2010) 21–24.
[24] A.E. Jansen, J.W. Assink, J.H. Hanemaaijer, J. van Medevoort, E. van Sonsbeek, Development and pilot testing of full-scale membrane distillation modules for deployment of waste heat, Desalination, 323 (2013) 55–65.
[25] M. Gryta, Effectiveness of water desalination by membrane distillation process, Membranes, 2 (2012) 415–429.
[26] M.I. Ali, E.K. Summers, H.A. Arafat, J.H. Lienhard V, Effects of membrane properties on water production cost in small scale membrane distillation systems, Desalination, 306 (2012) 60–71.
[27] E.K. Summers, H.A. Arafat, J.H. Lienhard V, Energy efficiency comparison of single-stage membrane distillation (MD) desalination cycles in different configurations, Desalination, 290 (2012) 54–66.
[28] S. Lin, N.Y. Yip, M. Elimelech, Direct contact membrane distillation with heat recovery: thermodynamic insights from module scale modeling, J. Membr. Sci., 453 (2014) 498–515.
[29] M. Gryta, Water purification by membrane distillation process, Sep. Sci. Technol., 41 (2006) 1–10.
[30] M.M. Teoh, S. Bonyadi, T.S. Chung, Investigation of different hollow fiber module designs or flux enhancement in the membrane distillation process, J. Membr. Sci., 311 (2008) 371–379.
[31] Z. Ju-Meng, X. Zhi-Kang, L. Jian-Mei, W. Shu-Yuan, X. You-Yi, Influence of random arrangement of hollow fiber membranes on shell side mass transfer performance: a novel model prediction, J. Membr. Sci., 236 (2004) 145–151.
[32] D. Zhongwei, L. Liying, M. Runyu, Study on the effect of flow maldistribution on the performance of the hollow fiber modules used in membrane distillation, J. Membr. Sci., 215 (2003) 11–23.
[33] J. Lemanski, G.G. Lipscomb, Effect of shell-side flows on hollow fiber membrane device performance, AIChE J., 41 (1995) 2322–2326.
[34] M.C. Richmond, W.A. Perkins, T.D. Scheibe, A. Lambert, B.D. Woodb, Flow and axial dispersion in a sinusoidal-walled tube: effects of inertial and unsteady flows, Adv. Water Resour., 62 (2013) 215–226.
[35] A. Ali, P. Aimar, E. Drioli, Effect of module design and flow patterns on performance of membrane distillation process, Chem. Eng. J., 277 (2015) 368–377.
[36] H. Yu, X. Yang, R. Wang, A.G. Fane, Numerical simulation of heat and mass transfer in direct membrane distillation in a hollow fiber module with laminar flow, J. Membr. Sci., 384 (2011) 107–116.
[37] K. Schneider, T.J. van Gassel, Membrane distillation, Chem. Ing. Technol., 56 (1984) 514–521.